

NREL/NWTC AERODYNAMICS CODE BLIND COMPARISON

September 7, 2000

Background

Earlier in the year, a substantial amount of accurate, well resolved full scale wind turbine data were acquired by testing the NWTC Unsteady Aerodynamics Experiment (UAE) in the NASA Ames National Full Scale Aerodynamics Complex 80' x 120' wind tunnel. An effort is currently in progress to assess the fidelity, robustness, and efficiency of existing wind turbine computational models by comparing model predictions with a select subset of these wind tunnel test results.

Comparisons will be conducted in two successive phases. In the blind comparison phase, modelers will predict turbine aerodynamic response based only upon wind tunnel conditions and turbine properties. In the subsequent calibrated comparison phase, modelers will be given a limited spectrum of turbine aerodynamics measurements with which to calibrate their models. Then, using calibrated models, participants will repeat predictions previously accomplished during the blind phase.

This document contains instructions and information intended to enable modelers to participate in this comparison exercise. To maximize the types of models represented in this effort, participants are being solicited from academe, government, and industry, both in the United States and abroad. This document, along with appropriate ancillary references, provides instructions and input data to those who wish to participate in this code comparison.

Configurations

Participants are asked to provide results for two UAE configurations. The first configuration consists of a rigid hub with the rotor located upwind of the tower, while the second comprises a rigid hub downwind of the tower. The blade flap angle, or pre-cone angle, differs between the upwind and downwind configurations. Specific wind speeds, blade pitch angles, and yaw errors are listed in Table 1 along with other pertinent information. The file naming convention uses the first character to designate the turbine configuration (S: upwind; E: downwind). The second and third characters specify the nominal wind speed. The next four characters specify the nominal yaw error angle with 'M' indicating negative yaw error. The last character differentiates between repeated data points.

Table 1. Input parameters for each turbine condition.

Filename	Blade Flap Angle (deg)	Tip Pitch Angle (deg)	Wind Tunnel Air Temperature (deg Celsius)	Yaw Angle (deg)	Rotational Speed (rpm)	Wind Speed (m/s)	Air Density (kg/m ³)
S0700000	0	3.0	11.1	0.0	71.9	7.0	1.246
S1000000	0	3.0	11.0	-0.0	72.1	10.0	1.246
S1300000	0	3.0	13.7	-0.0	72.1	13.1	1.227
S1500000	0	3.0	14.2	-0.0	72.1	15.1	1.224
S2000000	0	3.0	14.5	0.1	72.0	20.1	1.221
S2500000	0	3.0	14.4	-0.1	72.1	25.1	1.220
S1000100	0	3.0	10.9	10.0	72.1	10.1	1.246
S1300100	0	3.0	13.7	10.1	72.1	13.1	1.227
S1500100	0	3.0	14.2	10.0	72.1	15.1	1.224
S1000300	0	3.0	10.9	30.2	72.0	10.1	1.246
S1300300	0	3.0	13.7	30.0	72.2	13.0	1.227
S1500300	0	3.0	14.0	29.9	72.2	15.1	1.225
S1000600	0	3.0	10.9	60.0	71.7	10.1	1.246

S1500600	0	3.0	13.9	60.0	71.9	15.1	1.225
E070000A	3.4	3.0	11.7	0.1	71.9	7.0	1.234
E170000A	3.4	3.0	11.5	0.1	72.0	17.1	1.234
E070020A	3.4	3.0	11.7	20.0	71.9	7.1	1.234
E170020A	3.4	3.0	11.4	20.2	72.2	17.2	1.234
E07M020A	3.4	3.0	11.6	-19.9	71.9	7.0	1.235
E17M020A	3.4	3.0	11.4	-20.0	72.1	17.2	1.234

For the rigid, upwind configuration (file names beginning with S), 14 cases are listed, encompassing wind speeds from 7 to 25 m/s, and yaw angles from 0° to 60°. Zero yaw cases for wind speeds from 7 to 25 m/s represent conditions wherein the turbine blades operate continuously below or above static stall. Nonzero yaw cases correspond to conditions that drive blade angle of attack dynamically through the static stall. Table 1 lists 6 cases for the rigid, downwind configuration (file names beginning with E). Within this subset, the low wind speed corresponds to the subcritical Reynolds number regime, which commonly yields a cohesive vortex wake from the tower. The high wind speed lies in the supercritical Reynolds number range, yielding a generally disorganized wake. Both positive and negative nonzero yaw conditions prompt the blade to intersect the tower wake at high as well as low instantaneous angles of attack.

Model Output Data

For each of the 20 sets of conditions specified above in Table 1, participants are asked to provide the model outputs listed in Table 2, in the order shown. In addition to listing the quantities of interest, Table 2 specifies the units and sign convention that should be used. The output file format can be downloaded from the web-site. It is an Excel spreadsheet containing one sheet for each configuration in Table 1 corresponding to the filenames in the first column.

Table 2. Output parameters and measurement conventions.

Channel ID Code	Channel Description, Units	Measurement Convention
YAW	Yaw Angle (deg)	Positive clockwise viewed from above turbine. See Figure 1.
VTUN	Tunnel Speed (m/s)	
B3AZI	Blade 3 Azimuth angle (deg)	Clockwise viewed from downwind for downwind rotor; counter-clockwise viewed from downwind for upwind rotor. See Figure 2.
B3FLAP	Blade 3 Flap Angle (deg)	Positive downwind.
B3PITCH	Blade 3 pitch angle (deg)	See Figure 3
RPM	Rotational Speed (rpm)	
B3RFB	Blade 3 Root Flap Bending Moment (Nm)	Perpendicular to tip chord; positive downwind
B3REB	Blade 3 Root Edge Bending Moment (Nm)	Parallel to tip chord; positive in direction of rotation (See B3AZI above)
LSSTQ	Low-speed Shaft Torque (Nm)	Positive in direction of rotation (See B3AZI above)
NAYM	Nacelle Yaw Moment (Nm)	See Figure 6.
QNORM30	Local dynamic pressure at 30% span (Pa)	
QNORM47	Local dynamic pressure at 47% span (Pa)	
QNORM63	Local dynamic pressure at 63% span (Pa)	
QNORM80	Local dynamic pressure at 80% span (Pa)	
QNORM95	Local dynamic pressure at 95% span (Pa)	

CN30	30% span Normal Force Coefficient	See Figure 8.
CT30	30% span Tangent Force Coefficient	See Figure 8.
CM30	30% span Pitching Moment Coefficient	See Figure 8.
CN47	47% span Normal Force Coefficient	See Figure 8.
CT47	47% span Tangent Force Coefficient	See Figure 8.
CM47	47% span Pitching Moment Coefficient	See Figure 8.
CN63	63% span Normal Force Coefficient	See Figure 8.
CT63	63% span Tangent Force Coefficient	See Figure 8.
CM63	63% span Pitching Moment Coefficient	See Figure 8.
CN80	80% span Normal Force Coefficient	See Figure 8.
CT80	80% span Tangent Force Coefficient	See Figure 8.
CM80	80% span Pitching Moment Coefficient	See Figure 8.
CN95	95% span Normal Force Coefficient	See Figure 8.
CT95	95% span Tangent Force Coefficient	See Figure 8.
CM95	95% span Pitching Moment Coefficient	See Figure 8.
N30	30% span Normal Force (N/unit span)	
T30	30% span Tangent Force (N/unit span)	
M30	30% span Pitching Moment (Nm/unit span)	
N47	47% span Normal Force (N/unit span)	
T47	47% span Tangent Force (N/unit span)	
M47	47% span Pitching Moment (Nm/unit span)	
N63	63% span Normal Force (N/unit span)	
T63	63% span Tangent Force (N/unit span)	
M63	63% span Pitching Moment (Nm/unit span)	
N80	80% span Normal Force (N/unit span)	
T80	80% span Tangent Force (N/unit span)	
M80	80% span Pitching Moment (Nm/unit span)	
N95	95% span Normal Force (N/unit span)	
T95	95% span Tangent Force (N/unit span)	
M95	95% span Pitching Moment (Nm/unit span)	

Each wind tunnel data set consisted of 30 seconds of data, which corresponds to 36 rotor revolutions. A comparable simulation should be run, and the time series azimuth averaged in 1° bins (centered on the integer, i.e., 359.5 to 0.5 for the 0 degree bin) as indicated in the sample output file. In addition, the mean, standard deviation, maximum and minimum values for each channel should be included in the output file. In the top left cell, please insert your institution name as it should appear in the legend of the plots that will be made.

Documentation of Model and Inputs

In addition to the numerical data described above, participants are expected to provide a background summary of their model that includes, but is not limited to, the subjects listed below. Participants are encouraged to include figures, equations, tables, and graphs to enhance the clarity and completeness of these summaries. Separate summaries also will describe any changes made between the blind and calibrated phases of the comparison, and appropriate figures, equations, tables and graphs are again recommended. A short bibliography listing works that document code development and validation is also highly encouraged.

Domain discretization – Blade partitioning, lattice conformation, gridding/meshing, multidomain structuring, etc.

Model inputs – Experimentally obtained aerodynamic input data and sources, empirical modifications to experimental input data (tip and hub loss models, 3-D stall delay, etc.),

air density, air viscosity, inflow speed and profile, disk yaw error, blade pitch angle, blade RPM, empirically derived aerodynamic input tables and sources, etc.

Solution algorithm and physics – BEMT, lifting line, dynamic stall modeling, wake modeling, prescribed wake, free wake, finite difference, finite volume, finite element, transition and turbulence models for blade boundary layer, aerostructural coupling, rigid body dynamics, assumed mode dynamics, multi-body dynamics, etc.

Model assumptions and approximations – Steady flow, attached flow, potential flow, viscous-inviscid interaction, thin shear layer, Reynolds averaging, reconstruction order, regularization/homogenization, tunnel boundary effects, etc.

Performance attributes – Computer type, memory usage, CPU time to converge, set-up time and resources, etc.

Post processing – Derived/estimated outputs, interpolation/extrapolation, spatial averaging, time averaging, azimuth averaging, etc.

Submission of Results

Results should be submitted to NREL/NWTC by November 3, 2000 by e-mail. Please send completed Excel output files to david_simms@nrel.gov.

UAE Configuration Data

Complete information regarding UAE instrumentation and configuration can be found on the web-site. Additional modal test information such as frequency response functions and the coordinates of the collected data can be provided if requested. Measurement conventions for the requested channels are reproduced below on the following pages. Please note that most measurement conventions are referenced to the wind direction, and not the turbine tower. Therefore, when switching between upwind and downwind turbine configurations, the measurement conventions for most channels must be changed to remain oriented to the wind. For example, the blade root flap bending moment is positive in the downwind direction. Simply rotating the turbine from a downwind to upwind configuration will result in blade root flap bending moment positive upwind unless the convention is changed in the model.

Position Encoders

The yaw angle, instrumented blade (Blade 3) azimuth angle, blade pitch angles and blade flap angles were all measured with digital position encoders. The measurement conventions are shown in Figures 1-3.

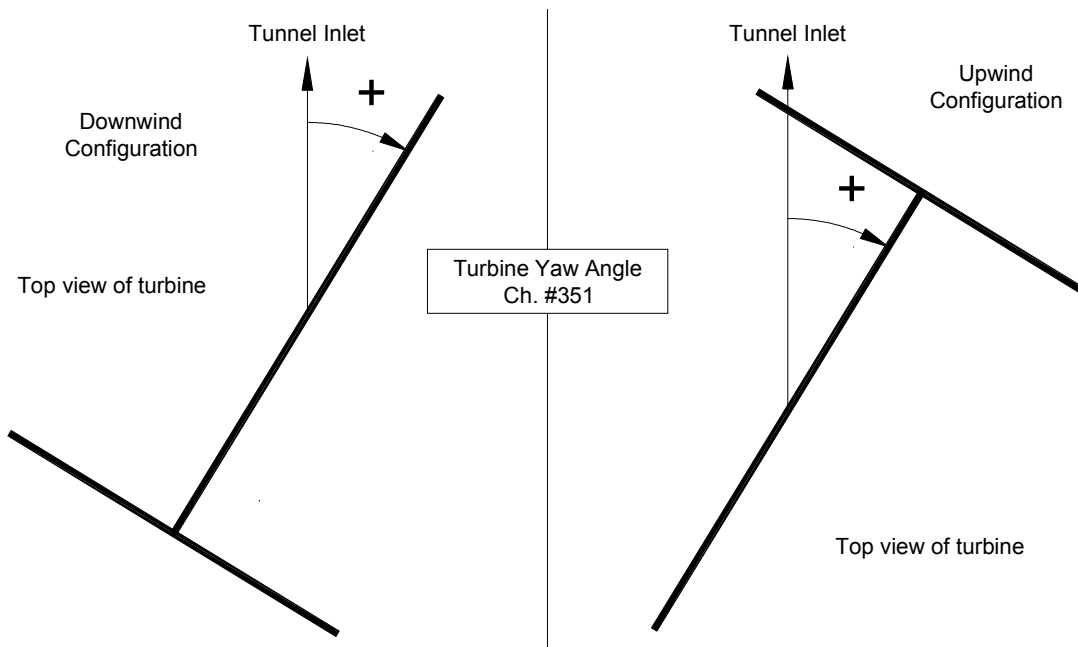


Figure 1. Yaw angle measurement convention.

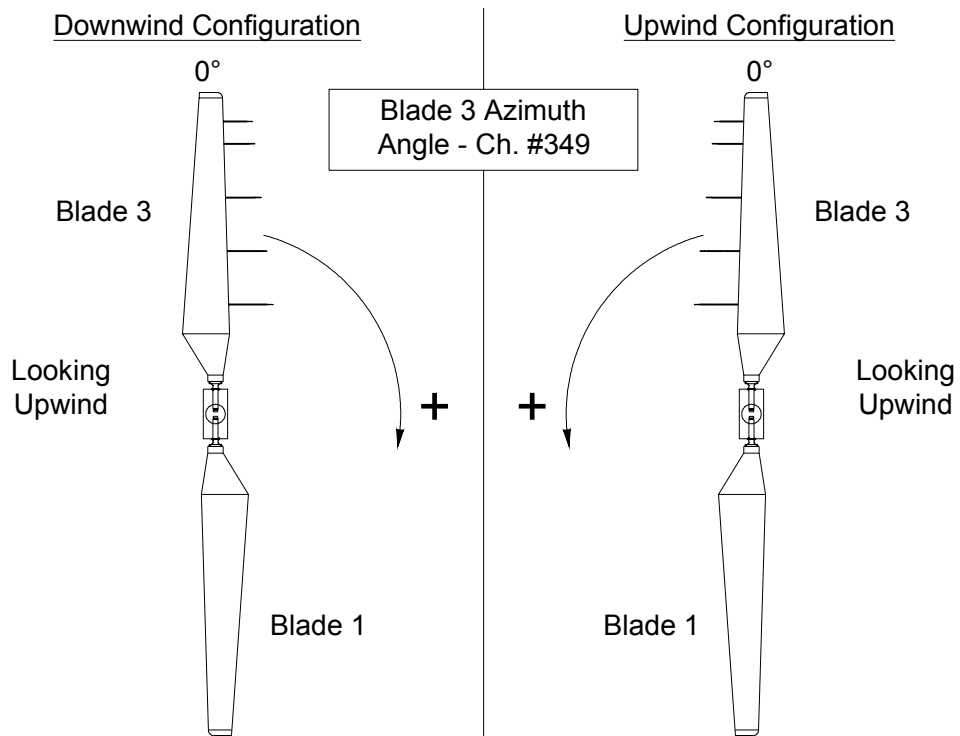


Figure 2. Rotor azimuth angle convention.

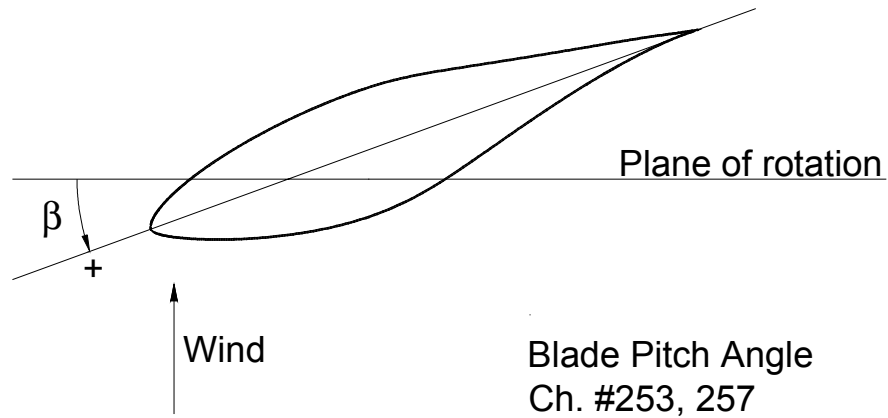


Figure 3. Blade pitch angle measurement convention.

Strain Gages and Load Cell

Bending moments were measured at the root of each blade and on the low-speed shaft with strain gages. The strain gages measuring root flap and edge loads were applied to the steel pitch shaft adjacent to the blade attachment location. The pitch shaft was reduced to a uniform, cylindrical, 80 mm diameter at 8.6% span, the location where the strain gages were applied. The uniform, cylindrical region eliminates geometry effects to facilitate accurate measurement of flap and edge bending moments. This cylindrical section of the blade root is illustrated in Figure 4. The gages were aligned with the chord at the tip of the blade. The rotor torque was measured with strain gages installed on the low-speed shaft as shown in Figure 5. The measurement conventions were such that positive blade root flap bending occurred in the downwind direction for both the upwind and downwind turbine configurations. Blade root edge bending and low-speed shaft torque were positive in the direction of rotation for both the upwind and downwind turbine configurations.

Side View

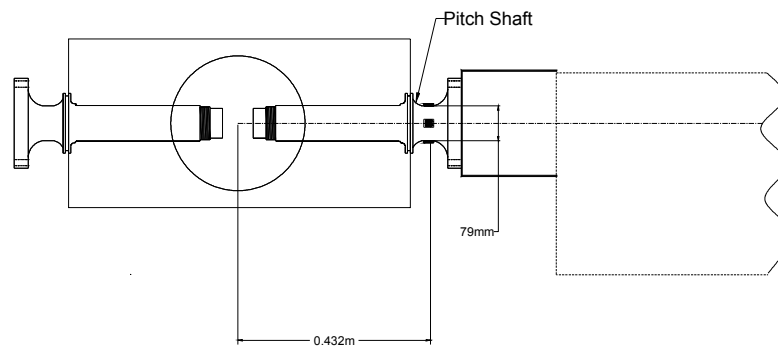


Figure 4. Blade root strain gage location.

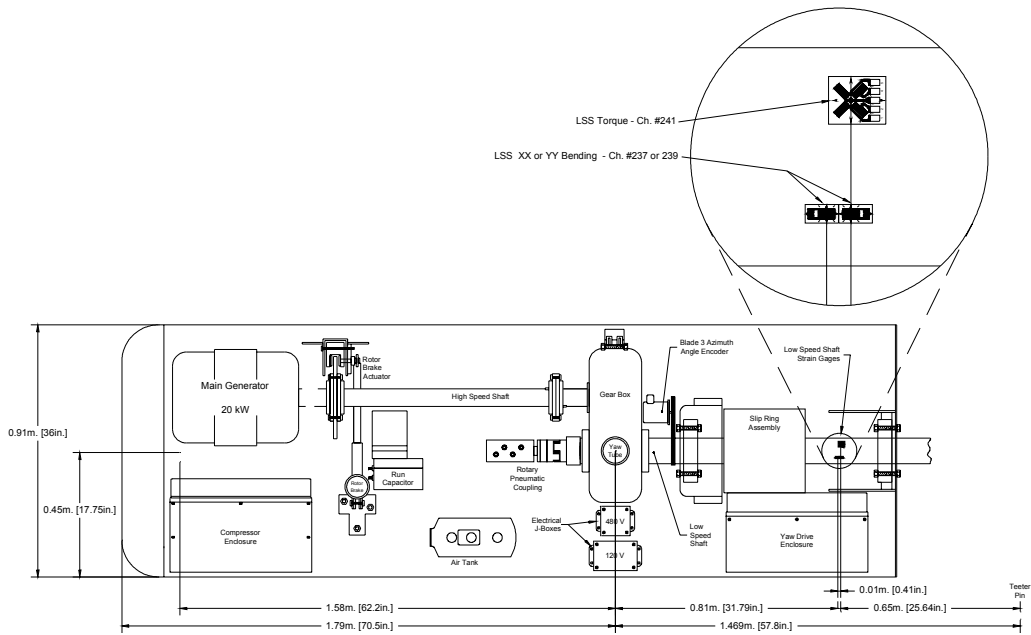


Figure 5. Low-speed shaft strain gage location within nacelle.

A tension/compression load cell was used to measure the yaw moment. The load cell was placed adjacent to the yaw brake caliper constraining the motion of 4-bar linkage where the brake caliper is one bar. Yaw moment was a positive moment in the direction required to restore the turbine from a negative yaw error to zero yaw error for both upwind and downwind turbine configurations as shown in Figure 6.

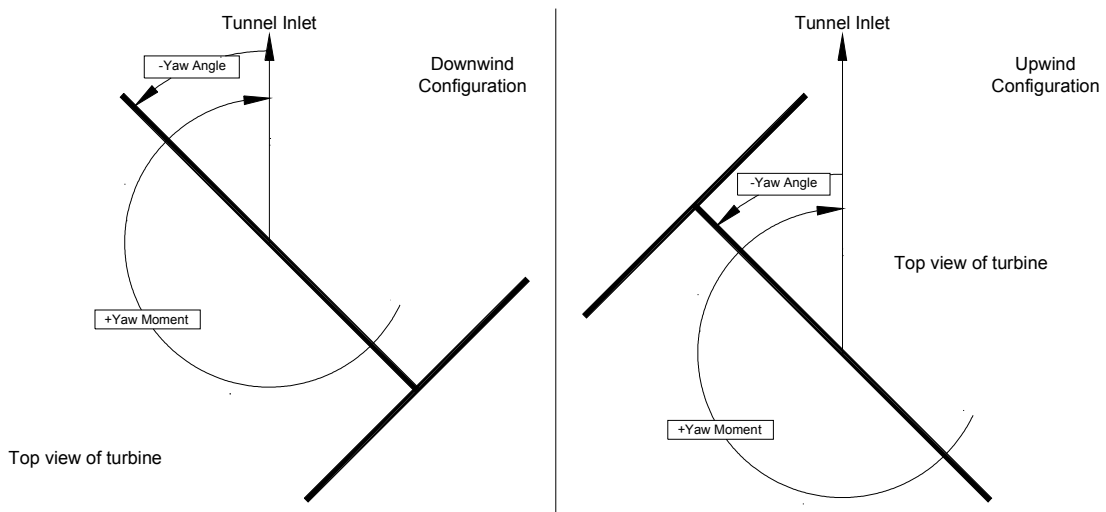


Figure 6. Yaw moment measurement convention.

Pressure Measurements

Aerodynamic coefficients for a particular radial station resulted from the integrated value of the measured pressure distribution at five span locations. The measurement approach was to install small pressure taps in the surface of the blade skin. Each opening was mounted flush to the airfoil surface. The flush profile was necessary to prevent the taps themselves from disturbing the flow. Stainless steel tubes with an outer diameter of 1.5875 mm (0.6731 mm inner diameter), were installed inside the blade's skin during manufacturing to carry surface pressures to the pressure transducer. A short piece of plastic tubing (0.6731 mm inner diameter) joined the tubes to the transducers. To mitigate potential dynamic effects, total tubing length was kept less than 0.45 m (18 in) by mounting the pressure transducers inside the blade near the pressure tap locations. The taps were aligned along the chord (instead of being staggered) so that span-wise variations in pressure distributions would not distort measured chordwise distributions. As illustrated in Figure 7, the taps were concentrated toward the leading edge to achieve increased resolution in the more active areas of the pressure distributions.

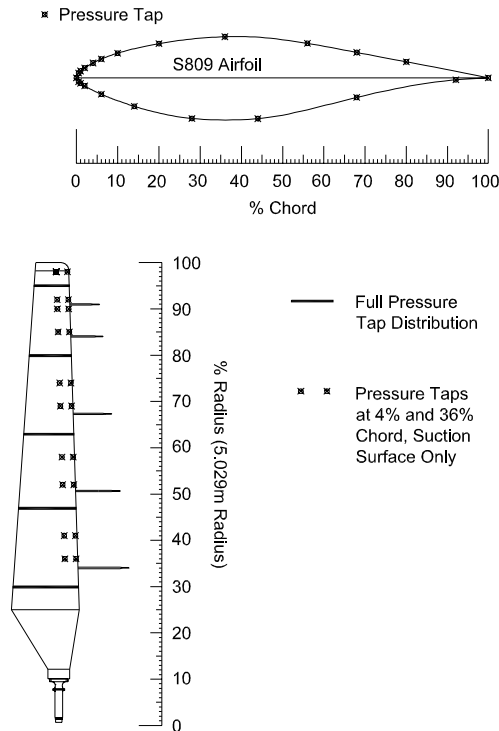


Figure 7. Blade surface pressure instrumentation.

Twenty-two taps were instrumented at five primary span-wise locations: 30% span, 46.6% span, 63.3% span, 80% span, and 95% span. Pairs of taps at 4% chord and 36% chord were installed at various other intermediate span locations (36%, 41%, 52%, 58%, 69%, 74%, 85%, 90%, 92%, and 98%) on the suction surface.

The pressure distributions for rotating-blade data were integrated to compute normal force coefficients (C_N) and tangential force coefficients (C_T). They represent the forces acting perpendicular and parallel to the airfoil chord, respectively. The average pressure between two adjacent taps was first projected onto the chord line, integrated to determine the C_N values, and then projected onto an axis orthogonal to the chord and integrated to compute C_T values. This

procedure is described in detail by Rae and Pope (1984). Equations (1) and (2) give the integration procedure used to determine C_N and C_T . The x and y values begin at the trailing edge ($x = 1$), proceed forward over the upper surface of the blade, and then aft along the bottom surface, ending at the starting point, the trailing edge.

$$C_N = \sum_{i=1}^{\#oftaps} \left| \frac{C_{p_i} + C_{p_{i+1}}}{2} \right| (x_{i+1} - x_i), \text{ and} \quad (1)$$

$$C_T = \sum_{i=1}^{\#oftaps} \left(\frac{C_{p_i} + C_{p_{i+1}}}{2} \right) (y_{i+1} - y_i); \quad (2)$$

where,

C_p = normalized pressure coefficient

x_i = normalized distance along chord line from leading edge to i^{th} pressure tap

y_i = normalized distance from chord line along axis orthogonal to chord to i^{th} pressure tap

In a similar integral procedure, pitching moment coefficients (C_M) were determined. The pitching moment represents the total moment about the 1/4 chord due to the normal and tangential forces at a pressure tap with the vertical or horizontal distance from the pitch axis as the moment arm. Note that the pitch and twist axis is at 30% chord, but the moment is computed about 25% chord. This equation follows:

$$C_M = - \sum_{i=1}^{\#oftaps} \left[\left(\frac{C_{p_i} + C_{p_{i+1}}}{2} \right) \left[(x_{i+1} - x_i) \left(\frac{x_{i+1} - x_i}{2} + x_i - 0.25 \right) + (y_{i+1} - y_i) \left(\frac{y_{i+1} - y_i}{2} + y_i \right) \right] \right]. \quad (3)$$

The measurement convention for the aerodynamic force coefficients is shown in Figure 8. The sectional normal force, tangent force, and pitching moment use the same measurement conventions. These can be computed by multiplying the force coefficient by the dynamic pressure and the chord length. An example for the normal force at 30% span follows:

$$N_{30} = Q_{NORM30} * C_{N30} * (0.711m) \quad (4)$$

The chord lengths for each of the pressure tap span locations are shown in Table 3.

Table 3. Pressure tap span locations and chord length.

Span Location	Chord Length (meters)
30%	0.711
46.6%	0.627
63.3%	0.542
80%	0.457
95%	0.381

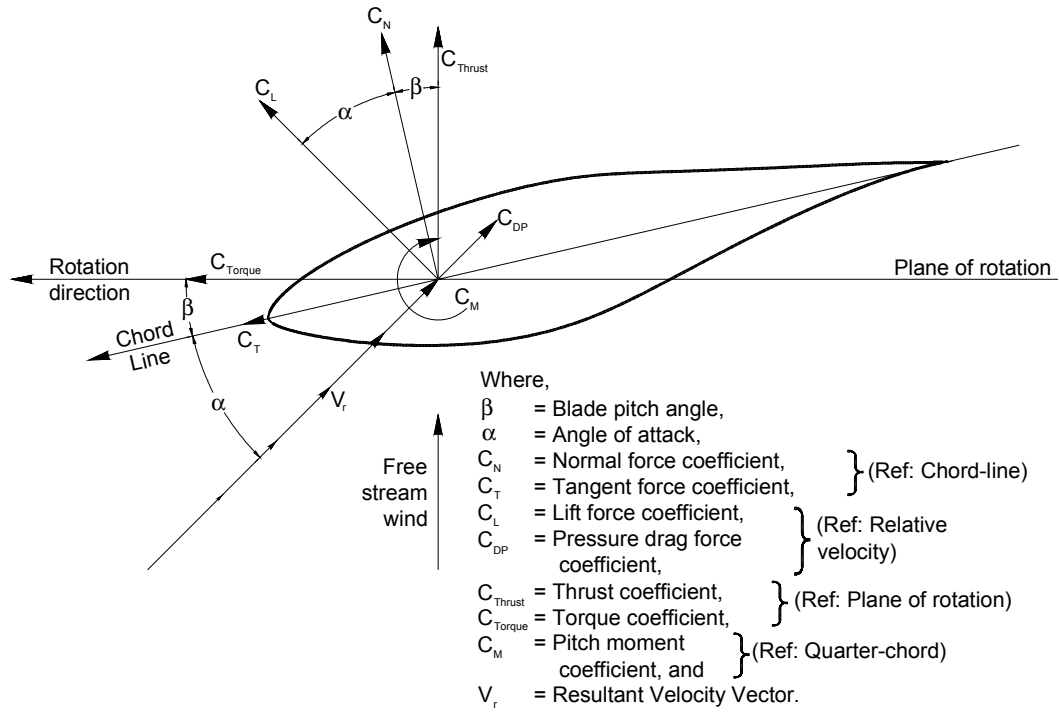


Figure 8. Aerodynamic force coefficient measurement convention.